Article

Using Graphene Field-Effect Transistors for Real-Time Monitoring of Dynamic Processes at Sensing Interfaces. Benchmarking Performance against Surface Plasmon Resonance

Juliana Scotto,[§] Agustín L. Cantillo,[§] Esteban Piccinini, Gonzalo E. Fenoy, Juan A. Allegretto,
José M. Piccinini, Waldemar A. Marmisollé,* and Omar Azzaroni

Cite This: ACS Appl. Electron. Mater. 2022, 4, 3988−3996

Read Online

ACCESS | Metrics & More | Article Recommendations | Supporting Information

ABSTRACT: Graphene field-effect transistors (gFETs) are promising tools for the development of precise and affordable techniques for the study of molecular binding kinetics, crucial in applications such as biomolecule therapies, drug discovery, and medical diagnostics. Nevertheless, determining the reliability and modeling the gFET signal for the monitoring of molecular binding and adsorption are still needed. Here, we prove that the gFET technology allows monitoring in real time the adsorption of both positive and negative polyelectrolytes, used as model charged macromolecules, using a low-cost portable gFET setup (Zaphyrus-W10), whose graphene channel was produced by reduction of graphene oxide. The gFET response is compared and validated against the surface plasmon resonance (SPR) technique. Remarkably, the electronic response is directly correlated with the mass adsorption, and very similar kinetic profiles are obtained for both techniques.

Moreover, the adsorption kinetics of a polyelectrolyte assembled in a layer-by-layer give evidence that, even at ionic strengths near to the physiological conditions, the electrostatic interactions can be sensed at large distances from the graphene surface (20-fold higher in comparison to the solution Debye length). Biasing the gFET with a Ag/AgCl coplanar gate electrode avoids capacitive current contributions from nonbinding phenomena and displays a transistor signal proportional to the adsorbed mass. Furthermore, a marked amplification of the electronic signal without alteration of the macromolecule adsorption kinetics by using a Ag/AgCl gate in comparison with a nongated device is evidenced. Thus, the suitability of the coplanar-gated gFET technology for the study of molecular binding kinetics is illustrated.

KEYWORDS: electrolyte-gated field-effect transistor (EG-FET), surface plasmon resonance (SPR), layer-by-layer (LBL), polyelectrolyte multilayer (PEM), graphene, macromolecules, binding kinetics, sensor
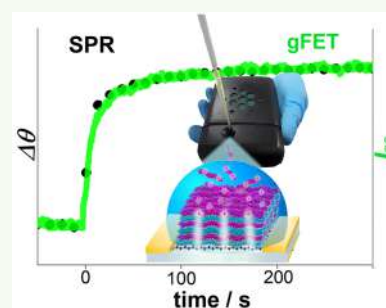
INTRODUCTION

In recent years, biotechnology has showed impressive advances through the discovery and use of novel receptors such as CRISPR-Cas, aptamers, and nanoantibodies, among others,[1−3] A broad number of applications, going from biomolecule therapies to drug discovery and the development of medical diagnostic tools, depend on the interaction of such receptors with their target ligand and their integration to functional interfaces.[2−6] Quantifying macromolecule binding to target ligands and *in situ* adsorption monitoring is critical to both fundamental research and innovative product development.[7] Thus, it becomes imperative to have access to efficient analytical techniques that allow characterizing and monitoring the evolution of interfaces at a molecular level. In particular, label-free techniques are especially interesting in order to simplify experimental procedures and avoid the perturbation of the binding interactions.[8,9] Among them, surface plasmon resonance (SPR) and bio layer interferometry (BLI) are two widely employed surface-sensitive techniques that are considered gold standards for the kinetic study of the formation of

nanointerfaces, as well as for the monitoring of recognition events.[8−11] However, these techniques usually require sophisticated instruments and high-cost assays, limiting their availability.[12]

Within this scenario, graphene-based field-effect transistors (gFETs) have arisen as a next-generation technology that combines high sensitivity and fast response with low-cost and easy-to-operate instrumentation.[13−16] Moreover, these devices have been shown to be an interesting choice for the real-time detection of molecules and biomarkers, while allowing miniaturization.[13,17−21] In addition, the use of gFETs for the study of the binding kinetics among biomolecules such as proteins, DNA, RNA, and ligands has also been evaluated.[22−24]

However, there are still some obstacles that need to be overcome in order to transfer this technology to the market.

In this regard, one of the main challenges in the development of gFET devices for sensing in biological samples is to overcome the Debye screening that is less than 1 nm under physiological conditions. Among the different approaches employed to surpass this issue, the modification of the graphene surface with polymer layers has been proven to be an effective strategy to decrease the screening effect due to a lower ion concentration inside the film,[22] allowing the detection and quantification of charged molecules at distances from the surface even 1 order of magnitude greater than the Debye length.[25−28] Nevertheless, to apply this strategy to the kinetic study of binding events, some crucial aspects have to be considered. For instance, when molecules are adsorbed within a polymer environment, counterion accumulation leads to the formation of an electrical double-layer (EDL) capacitance that is accompanied by changes in the ion concentration and the water content inside the film, giving rise to modulations in the interface potential.[25,26,29] Due to this capacitive contribution, the correlation between the changes in the surface charge density and the molecule adsorption process over time is nontrivial and performing an accurate analysis of the gFET current with temporal resolution may be complex.[29]

In order to clarify this matter, a device for the simultaneous determination of surface mass and charge density changes was recently designed by combining SPR and gFET measurements.[29] Employing the gold SPR substrate as the gate terminal of the gFET, the growth of a polyelectrolyte multilayer (PEM) was monitored and it was stated that the gFET output current had a capacitive contribution, generated by the formation of an EDL, whose kinetic behavior was limited by slow ion diffusion through the PEM, hampering a direct correlation between the current and the mass adsorbed on the sensor surface. In that study, the gFET response took 15 times longer than that observed by SPR measurements, which has been ascribed to the occurrence of a second process subsequent to the polyelectrolyte adsorption related to the EDL dynamics on the PEM−solution interface. It is relevant to note here that the magnitude of the EDL capacitive contribution in the output current of gFET devices depends, on one hand, on the interface and solution properties and, on the other hand, on the gFET characteristics (gate features, electrode arrangement, drain−source potential, etc.).[30−32] Thus, to guarantee an accurate correlation between the gFET signal and the adsorption process, not only is a rational design of the interface architecture required but also an optimized measurement setup is needed together with a thorough analysis of the results.

In this work, we present a gFET device fabricated with a conducting channel obtained by reduction of graphene oxide and a coplanar Ag/AgCl gate electrode and demonstrate its capability to monitor the adsorption of charged macromolecules in real time, avoiding capacitive gating effects that delay the current response. To this end, we first monitored the layer-by-layer (LbL) assembly of poly-(diallyldimethylammonium chloride) (PDADMAC) and poly-(styrenesulfonate) (PSS) on a graphene substrate by SPR. Next, we built the same assembly on a gFET device while measuring the current changes in an open-circuit setup, demonstrating that the electrostatic interactions between adsorbed charges and the graphene channel can be sensed at large distances from the surface (20 times the solution Debye

length), even in a nongated system. Subsequently, we show that the current response can be amplified by applying a constant gate voltage without altering the response time. In addition, we performed a detailed study of the kinetic adsorption process by a comparative analysis of the SPR and gFET signals during the assembly and demonstrated that the gFET response over time can be directly correlated with the mass adsorption. Finally, the setup developed here allows continuous measurement of the polyelectrolyte assembly on the surface along several sequential deposition cycles, providing a very reliable monitoring of the adsorption kinetics by employing a much simpler, straightforward, and less expensive technique in comparison to SPR and BLI.

■ MATERIALS AND METHODS

Surface Plasmon Resonance (SPR) Spectroscopy. SPR102 Au substrates (BioNavis) were modified with cysteamine and then with reduced graphene oxide (rGO) as previously reported.[25,33] Then, in order to confer a negative charge to the surface, the rGO-modified substrates were incubated in a 5 mM sodium pyrene-1-sulfonate (PySO$_3$Na, Sigma-Aldrich) solution in dimethylformamide (DMF, Anedra), washed with pure DMF, and dried with N$_2$. The sequential adsorption of PDADMAC (M_w = 100.000−200.000 Da) and PSS (M_w = 70.000 Da) was monitored with an SPR Navi 210 A multiparametric surface plasmon resonance (MP-SPR) instrument (BioNavis Ltd., Tampere, Finland) employing lasers with 670 and 785 nm wavelengths. To this end, 0.1 mg/mL polyelectrolyte in 0.1 M KCl (Anedra) solutions were manually injected under nonflow conditions and the SPR angular scans were recorded for 10 min, followed by rinsing with 0.1 M KCl for 5 min. Winspall software (Max-Planck-Institute for Polymer Research, Mainz) was used to model the system and to fit the SPR experimental curves.

gFET Measurements. Graphene-based field-effect transistors produced by *in situ* reduction of graphene oxide (Model GFET-GB10) with a coplanar Ag/AgCl gate prepared by a previously reported scalable method were supplied by GISENS BIOTECH (Argentina).[34] A Zaphyrus-W10 FET measurement station (GISENS BIOTECH) was employed for field-effect electrical measurements. Before starting the LbL assembly, the rGO-FETs were modified with PySO$_3$Na following the same procedure described for the SPR substrate functionalization. Then, the modified substrates were placed in the cell and 200 μL of 0.1 M KCl solution was added. Transfer characteristic curves of each gFET were obtained by measuring the current between the drain and source electrodes (I_{DS}) as a function of the applied gate potential (V_G), while the potential difference between drain and source (V_{DS}) was fixed at 50 mV. Next, the PEM assembly was performed under the same conditions as the SPR measurements and the current during the polyelectrolyte deposition was measured in two different setups: (i) open-circuit measurements (OC-gFET), where a 50 mV fixed V_{DS} was applied and the I_{DS} was registered, leaving the gate terminal unplugged; (ii) electrolyte-gated measurements (EG-gFET), where a gate potential of −250 mV and V_{DS} = 50 mV were fixed as the I_{DS} current was measured (see the Supporting Information). For both setups, the experimental procedure to build the LbL assembly was as follows: first, 200 μL of 0.1 mg/mL (or 0.01 mg/mL) PDADMAC in 0.1 M KCl solution was added and the current was measured for 10 min. Then, the polyelectrolyte solution was removed from the cell and replaced by the same volume of 0.1 M KCl without interrupting the current acquisition. This washing step was repeated three times. Next, the same procedure was carried out by employing a PSS 0.1 mg/mL (or 0.01 mg/mL) in 0.1 M KCl solution. This sequence was repeated until a six-bilayer assembly was achieved. Measurements from each layer are labeled hereinafter as L1, L2, etc.

■ RESULTS AND DISCUSSION

SPR Monitoring of PEM Formation on rGO Substrates. PEMs were prepared by alternate deposition of positively charged PDADMAC and negatively charged PSS on top of rGO surfaces using the LbL technique, while monitoring the adsorption processes by SPR measurements. The changes in the minimum reflectance angle ($\Delta\theta_{min}$) were recorded during the assembly, and the variations in the internal reflection angle ($\Delta\theta_{tir}$) were subtracted from $\Delta\theta_{min}$ to eliminate the influence of bulk refractive index changes. In Figure 1A, the differences between those magnitudes, from
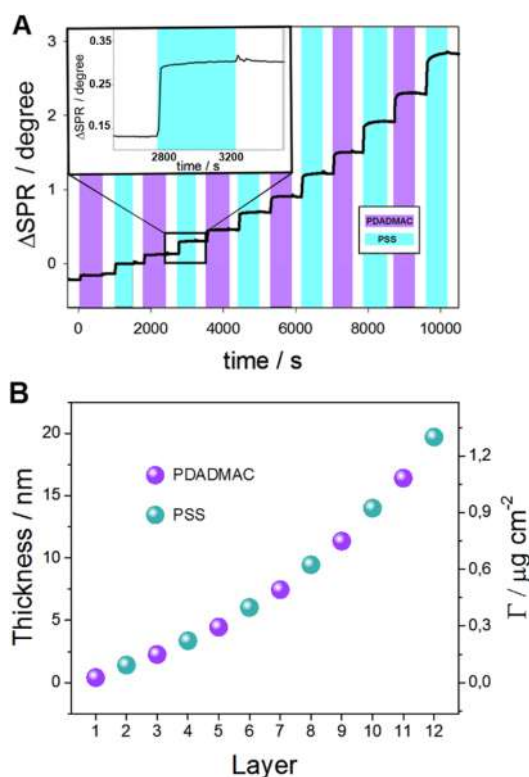

Figure 1. (A) ΔSPR ($\Delta\theta_{min} - \Delta\theta_{tir}$) during the assembly of a PDADMAC/PSS multilayer on top of rGO-modified Au sensors from 0.1 g/mL in 0.1 M KCl solutions. (B) Thickness of the assembly and mass surface densities, Γ, estimated from SPR measurements, as a function of the layer number.

now on referred as ΔSPR, are shown as the polyelectrolyte layers are assembled on the substrate. A rapid increase in the signal for both polyelectrolytes can be observed (90% of the adsorbed mass is deposited in less than 2 min for all layers), and no variation in ΔSPR is seen after each rinsing step, indicating the high stability of the assembly.

The surface coverage and the thickness of the PEM were estimated by fitting the reflectivity curves at 785 nm of the substrate (see details in the Supporting Information).[25] A supralinear growth of the assembly was found, as shown in Figure 1B. These results are in agreement with others previously reported for the PDADMAC/PSS assembly under similar experimental conditions.[29] Next, the monomer density adsorbed in each layer, $\Gamma_n(N)$, was estimated and the ratio $(\Gamma_n(N))/(\Gamma_n(N-1))$ was calculated.[34] The ratio obtained between the amounts of monomer adsorbed in each PSS layer with respect to the amount of monomer adsorbed in the previous PDADMAC layer, $((\Gamma_n(PSS,N))/(\Gamma_n(PDAD-$

MAC,$N-1$)), was found to be constant throughout the whole assembly process (~1 in average). For PDADMAC deposition, an average ratio of $(\Gamma_n(PDAMAC,N))/(\Gamma_n(PSS,N-1)) \approx 1.3$ was found, which is the origin of the supralinear behavior, widely reported for this system.[35−37] A possible explanation for this behavior is that, during PDADMAC adsorption, part of the chains adsorb directly onto the previous PSS layer through an intrinsic charge compensation mechanism and part of the chains form tails or loops into the solution that are extrinsically compensated by anions.[36] It has been proposed that these chains can diffuse through the PEM, leading to an internal reorganization of the assembly,[38] as will be discussed later. However, it is observed that both values are very close to unity, indicating that the charge compensation mechanism during the whole assembly is mainly intrinsic.[36] On the basis of these results, for the analysis of the correlation between the polyelectrolyte adsorption and the gFET measurements performed in the next sections, the PEM will be considered as a neutral film (inner layers) with the overcompensation charge density being located at the outermost polyelectrolyte layer, as reported elsewhere.[22]

gFET Monitoring of Polyelectrolyte Adsorption: Effect of the Gate Electrode on the Current Signal. PDADMAC/PSS multilayers were assembled on gFETs, employing the same conditions as those employed for the SPR measurements, and the current response during the growth of the PEM was studied. When a potential difference is applied between the drain and source terminals of the gFET (V_{DS}), a current in the graphene channel proportional to the carrier density in the channel is obtained. Next, the adsorption of polyelectrolytes on the sensor surface induces a modulation of the electric field that depends on the number and sign of the charges adsorbed, and consequently a change in the output current of the device is registered.[20] On the other hand, the charges on the outer layer generate an electrical double-layer capacitance due to counterion accumulation. Moreover, in the case of EG-gFETs, the existence of the EDL on the gate electrode should be also considered, and the magnitude of this contribution critically depends on the features of the gFET, such as size and material of the gate electrode, and distance between the graphene surface and the gate.[31,32]

In order to evaluate the influence of the gate capacitance in the gFET signal, the current changes during the PEM assembly were measured in two different configurations. In the first one, a two terminal (drain and source) setup was used, leaving the gate electrode unplugged. This configuration will be referred to as open-circuit gFET (OC-gFET). In the second configuration, a coplanar Ag/AgCl gate was added to the gFET (see the scheme in Figure 2A) and a gate voltage of −250 mV was applied. This configuration will be referred to as electrolyte-gated gFET (EG-gFET). In both configurations, a fixed V_{DS} of 50 mV was applied and the current between these two terminals, I_{DS}, was measured as the PEM was assembled. Baseline-subtracted results obtained with the two configurations are shown in Figure 2B,C.

When the results obtained for the OC-gFET configuration are analyzed, it is observed that the initial current value indicates that the open circuit potential of the sensor is near the charge neutrality point (V_{CNP}) (see Figure S2). Under this condition, a small change in the current with the adsorption of the polyelectrolytes should be expected because of the low transconductance in this region. Nonetheless, well-defined current changes were observed for both polyelectrolyte
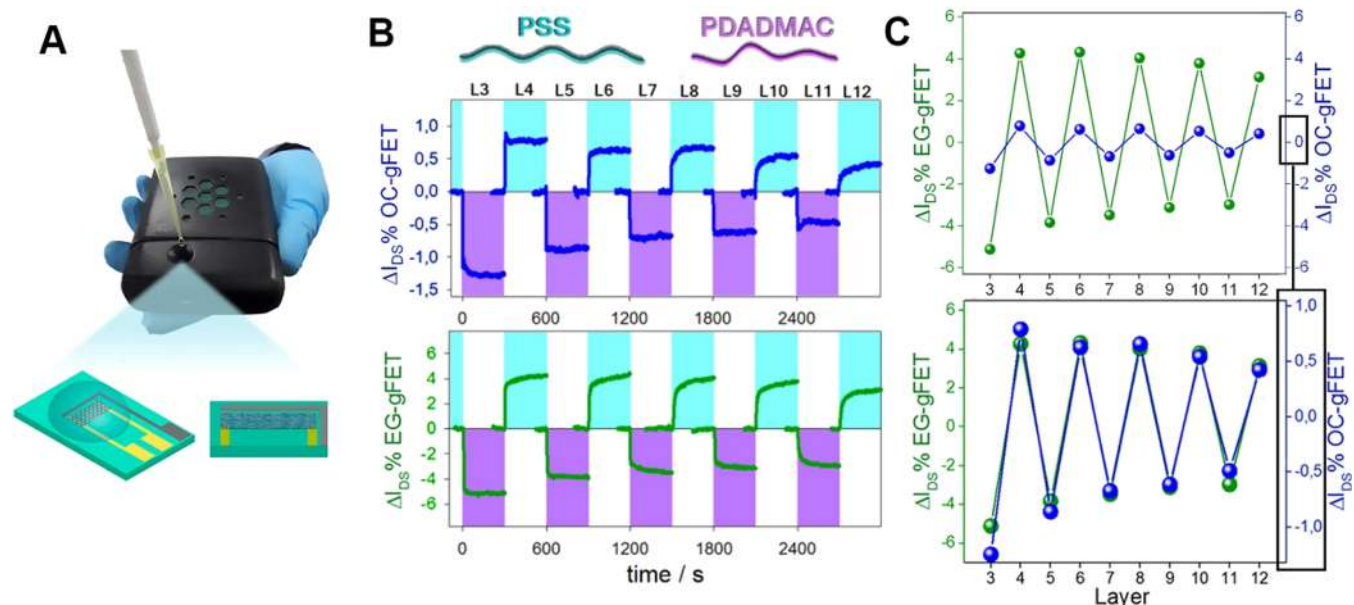
Figure 2. (A) Photograph of the FET measurement station Zaphyrus-W10 employed in this work and scheme of a gFET sensor. (B) Relative changes in the drain-source current (ΔI_{DS}%) for V_{DS} = 50 mV during the assembly of the PDADMAC/PSS multilayer measured with the OC-gFET (top) and with the EG-FET (bottom) (V_G = −250 mV). A linear baseline was subtracted from the original measurements by extrapolating the linear behavior of the current 2 min before the injection of the polyelectrolyte solution (see original curves in Figures S2B and S3B). (C) Current change achieved upon polyelectrolyte adsorption as a function of the layer number measured with the OC-gFET (blue) and the EG-gFET (green) configurations.

adsorption events. In Figure 2B, the relative changes in the current over time, ΔI_{DS}%, are plotted for each layer (ΔI_{DS}% = $\Delta I_{DS}/I_{DS}(0) \times 100$, where $I_{DS}(0)$ is the current before the injection of the polyelectrolyte solution). The adsorption of positively charged PDADMAC leads to a decrease in the current, indicating that the gFET is operating in a hole-carrier-dominated regime.[39] Upon PSS deposition, charge over-compensation generates an increase in the current induced by the adsorption of the negatively charged chains. This behavior is observed for all of the studied layers. However, a decrease in the magnitude of the current changes is observed as the layer number increases (Figure 2C), due to the electric potential decay across the film (see section S.4 in the Supporting Information).

In the EG-gFET configuration, the applied V_G = −250 mV sets a hole-carrier-dominated regime in the channel (see Figure S3A). Then, the adsorption of the positively charged PDADMAC leads to a decrease in the I_{DS} current due to a diminution of the number of positive charge carriers within the graphene channel. This effect can be also confirmed by a shift of the V_{CNP} to lower potential values in the transfer characteristic curves.[25] Oppositely, the adsorption of negatively charged PSS generates an increase in the current response for the same gating regime (Figure 2B, bottom panel). In this sense, these changes in the current should be the opposite with V_G potentials in the electron-carrier-dominated region (see section S.3 in the Supporting Information). A comparison of the maximum relative current changes obtained with the two sets of measurements are shown in Figure 2C. It can be appreciated that the magnitude of the current change measured with the EG-gFET configuration is about 5 times higher than that measured with the OC-gFET configuration. The higher response of the EG-gFET configuration arises from the fact that the applied V_G sets the channel in a region of high transconductance; thus, higher variations in the current can be obtained after the adsorption of a given charged polymer in comparison with the open-circuit configuration.

Beyond the difference in the amplitude of the response, the results obtained with the two configurations are very similar. As it can be seen in Figure 2B,C, for all of the assembly steps studied here (up to 12 layers), the adsorption of PDADMAC and PSS generates changes in the current in opposite ways, according to the charge of each polyelectrolyte layer. Moreover, the amplitude of the current variations caused by the polyelectrolyte adsorption decreases as the number of layer increases (and the thickness of the film does) in an identical fashion for both measurement configurations (see Figure 2C, bottom). This indicates that the application of the gate potential would not be affecting the physicochemical aspects of the LbL assembly, as the readout signals are identical in relative terms. Furthermore, the time variation of I_{DS} follows the same kinetic behavior for both gated and nongated setups. As an example, the normalized current variations for the gated mode and the open-circuit configuration during the deposition of the 10th layer (PSS) are shown in Figure 3. It can be seen that the kinetic responses overlap. This match between the kinetic profiles obtained with the two configurations is observed for all the layers studied here (see other curves in Figure S4). Moreover, it can also be observed that the time required to achieve the maximum current slightly increases with the layer number in the same manner for gated and nongated measurements. The similarities observed when the polyelectrolyte adsorption is monitored by both gFET configurations strongly suggest that no gating effects are operating on the LbL assembly process. This would imply that the gate potential does not markedly affect the kinetics of the sensing response when charged macromolecules interact with the functionalized graphene surface. In addition, we studied the effect of changing the polyelectrolyte concentration in the adsorption kinetic profile employing both gFET configura-
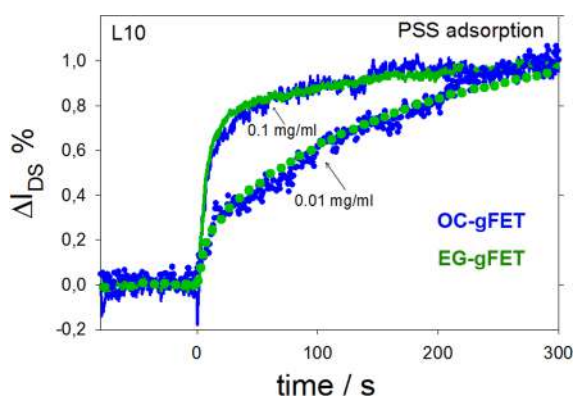
Figure 3. Normalized current changes in the gFET current during the deposition of the 10th layer (PSS) obtained with the OC-gFET (blue) and the EG-gFET (green) configurations for the assembly from different polyelectrolyte concentrations.

tions. As expected,[40] employing a lower polyelectrolyte concentration (0.01 mg/mL) yielded a slower deposition. Interestingly, the decrease in the deposition rate is equally observed by the two gFET configurations. In Figure 3, the normalized current changes for the deposition of the 10th layer of PSS from the 0.01 mg/mL solution are compared with the corresponding changes from the 0.1 mg/mL solution (the complete study is shown in the Supporting Information).

This match between both device configurations gives further evidence that introducing a coplanar Ag/AgCl gate electrode does not modify the kinetic profile of the gFET response, in contrast with other results obtained for the same assembly employing a gFET with a PEM-functionalized floating gold gate, where the EG-gFET kinetic studies mismatched with the OC-gFET studies.[29] In that case, the authors attributed the delay observed in the EG-gFET response to the formation of a double layer that modulates the local electric field. In the present case, this additional contribution to the gFET signal is not observed. Differences could arise from the fact that the gate electrode in this work is a true Ag/AgCl reference electrode that is not functionalized by the PEM deposition. Moreover, we measured the current between the gate and the source terminals (I_{GS}) during the assembly and found no changes in the current as a consequence of polyelectrolyte adsorption (see Figure S3C), suggesting that the effective working potential is not affected by modulations on the gate capacitance and that the I_{DS} response is defined by the physicochemical aspects of the binding interaction between the

charged macromolecules and the surface. To further explore these ideas, the capability of the gFET response for monitoring the LbL assembly is compared with the SPR method in the next section.

Correlation between the gFET Signal and the Mass Adsorption. To correlate the gFET response with the mass adsorption processes, a comparative kinetic analysis of the SPR and gFET responses was performed. As was shown before, the EG-gFET and OC-gFET configurations provide the same kinetic profile for the monitoring of the polyelectrolyte adsorption during the LbL assembly. Since the EG-gFET has a better sensitivity due to a greater amplitude of the signal, the results obtained with this configuration were chosen to perform a comparison with the SPR results.

It has been proposed that two different kinetic processes are involved in the adsorption of the polyelectrolyte layers during LbL assembly.[35] The first is associated with a fast adsorption step, which involves diffusion of the polyelectrolytes from the bulk to the surface and their adsorption driven by electrostatic interactions between the oppositely charged chains. The second involves a slower process, which is characterized by an internal reorganization of the film that implies the interdiffusion of polyelectrolyte chains into the PEM. The characteristic time associated with these processes depends on the assembly conditions, such as ion strength, polyelectrolyte concentration and molecular weight, the nature of the counterions, and the pH, among others.[40−44] Within this model, the mass density adsorbed as a function of time, t, can be expressed as[35]

$$\Gamma = \Gamma_1(1 - e^{(-t/\tau 1)}) + \Gamma_2(1 - e^{(-t/\tau 2)}) \tag{1}$$

where Γ_1 and Γ_2 represent the maximum mass densities adsorbed in each process and τ_1 and τ_2 are the characteristic times. Moreover, $\Gamma_1 + \Gamma_2 = \Gamma_T$, where Γ_T is the total adsorbed mass density at equilibrium.

Since the change in the mass surface density is proportional to the change in the minimum reflectance angle for the SPR signal (see eq S1), the ΔSPR curves were fitted to a double-exponential equation (Figure S6), and the fitting parameters are given in Table S1 in the Supporting Information. In Figure 4A, the τ_1 and τ_2 values are shown for the different layers (black stars and circles, respectively). From this analysis it appears that the first process (which involves the deposition of the largest amount of polyelectrolyte mass) has τ_1 values lower than 12 s for all layers studied here, in agreement with other studies.[35] The second process, associated with chain rearrange-
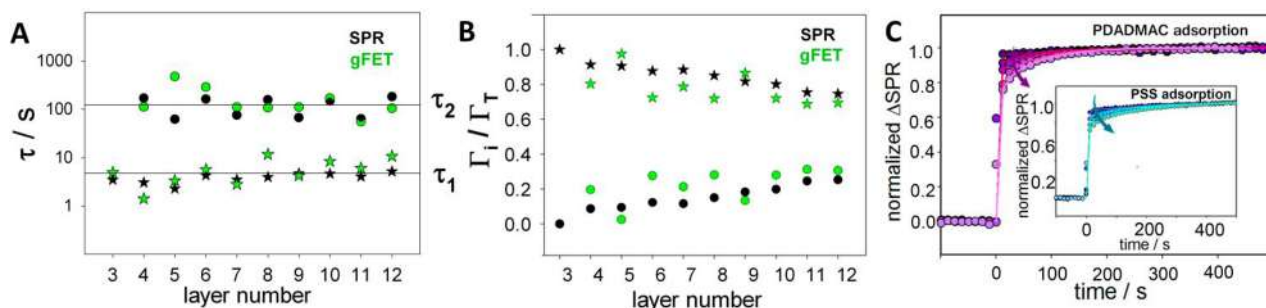

Figure 4. (A) Fitted τ_1 and τ_2 values (stars and dots, respectively) for a double-exponential behavior of the SPR and EG-gFET responses. (B) Relative contributions of the two processes to the total mass density. (C) Normalized SPR responses during PDADMAC layer deposition (circles) and the fitted exponential curves (lines). The arrow indicates the direction of the increasing number of layers. Inset: the same plots for PSS adsorption.
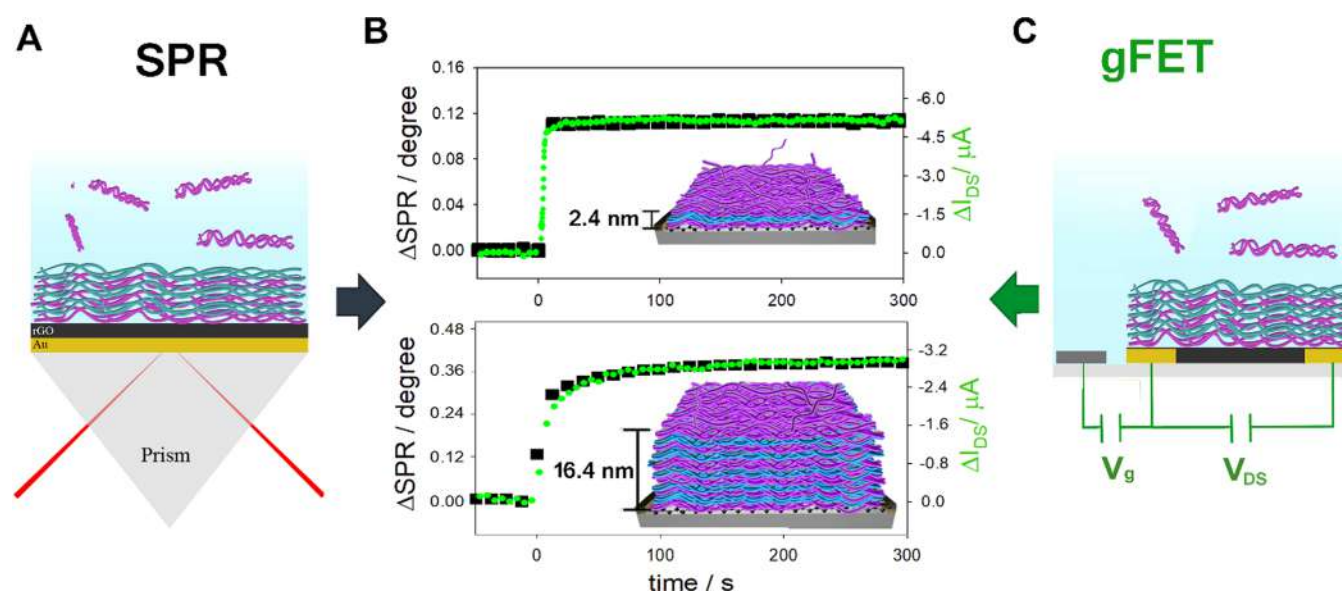
Figure 5. (A) Scheme of the SPR measurement setup. (B) Comparison of the ΔSPR curves (black squares) with the EG-gFET signal (green circles) for the adsorption of PDADMAC (3rd and 11th layers). (C) Scheme of the EG-FET measurement setup.

ment and diffusion through the PEM, has larger τ_2 values; therefore, the SPR signal requires a few minutes to reach a constant value. Moreover, it is observed that the relative contribution of this second process to the total mass deposited increases with the layer number (Figure 4B). As a consequence, a slower deposition is observed as the PEM thickness increases. For the sake of comparison, Figure 4C shows normalized SPR sensorgrams for the adsorption of both PDADMAC and PSS layers during the LbL assembly.

Next, the same analysis was carried out for the LbL assembly on a gFET monitored using the EG configuration. The values for the corresponding time constants obtained for a double-exponential fit are reported in Table S2 in the Supporting Information. In Figure 4A,B, the τ values and the fraction of the signal contribution for each process obtained from the EG-gFET response were added for comparison with those obtained from the SPR measurements. It can be seen that the parameters obtained with both techniques are coincident. When they are taken altogether, these results indicate that the gFET device is able to monitor both adsorption processes in a way similar to that of the more complex SPR technique. Furthermore, in Figure 5, the same kinetic behavior can be appreciated for the SPR and gFET signals, even when adsorption takes place at large distances from the electrode. Note, however, that the absolute mass adsorption cannot be determined from the gFET measurements, as is possible using a calibrated SPR setup.

The capability of gated-gFET devices to sense the adsorption of charged macromolecules beyond the Debye length has been explained through different mechanisms.[45] In the case of PEM assemblies, it has been proposed that there is a lower ion concentration inside the film that reduces the Debye screening, increasing the sensing range by 1 order of magnitude.[25] In the present case, a salt concentration of 0.1 M yields a Debye length of 0.96 nm in the bulk solution. However, changes in the current as the charged polymers are adsorbed can be observed even at ∼20 nm from the surface. This result can be explained by the lower decay of the electric

potential, ψ, inside the film in comparison with its behavior in solution (see Scheme 1 in the Supporting Information).

The direct correlation between the SPR signal and the gFET current response over time shows that, for each polyelectrolyte layer adsorbed at a certain distance from the electrode surface, $\Delta I_{DS}\%$ is proportional to Γ. On the other hand, $\Delta I_{DS}\%$ decreases as the distance between the adsorption process and the graphene surface, x, increases. Both behaviors can be explained by employing the Debye−Hückel model. As has been previously shown,[25] the decay of the surface potential inside the film can be accounted for as

$$\psi(x) = \psi_0 e^{(-x/\lambda)} \tag{2}$$

where ψ_0 is the potential at the PEM/solution interface and λ is the Debye length inside the film. Considering that ΔI_{DS} is proportional to ΔV_{CNP}, and that ΔV_{CNP} is proportional to the potential changes on the graphene surface ($\Delta\psi_g$),[39] then the current changes generated by the adsorption of a polyelectrolyte layer of mass density Γ at a distance d to the electrode can be written as

$$\Delta I_{DS} = A'\Gamma e^{(-d/\lambda)} \tag{3}$$

where A' is a proportionality constant (see section S.4 in the Supporting Information). By combining gFET and SPR data, the ratio $\Delta I_{DS}/\Gamma$ can be computed for each polyelectrolyte layer. In Figure 6, $\ln((|\Delta I_{DS}|)/\Gamma)$ is presented as a function of the PEM film thickness, d. According to eq 3, the slope of this plot allows obtaining the effective Debye length inside the LbL film. From the linear fitting, an average value of $\lambda = 10.3$ nm inside the polymer film was obtained under the experimental conditions employed in this work. This result is much higher than the value expected for the bulk solution (0.96 nm), and it is in excellent agreement with previous works that suggest a 1 order increase in the Debye length when the charges are separated from the surface by a neutral polyelectrolyte blend film.[25] Notably, the extended length for charge detection found here reaches the dimensions of many surface architecture designs for biomolecular recognition,[46−49] indicating the potential of this technology for the study of the kinetics of
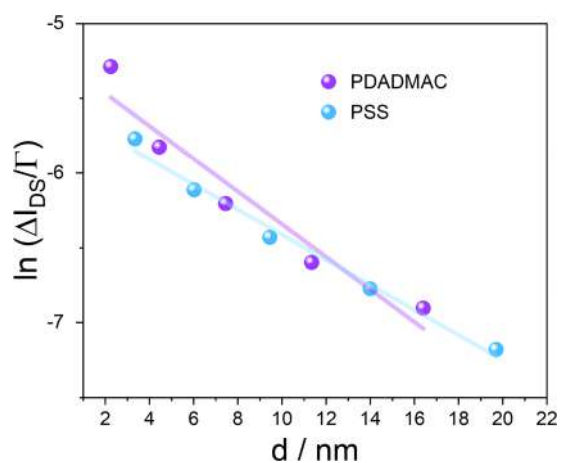
Figure 6. $\ln\left(|\Delta I_{DS}|/\Gamma\right)$ as a function of the distance between the plane where adsorption takes place and the graphene sensing surface, which corresponds to the PEM film thickness. The fitting corresponds to eq 3 (see the Supporting Information).

binding interactions and the determination of receptor–ligand affinity constants.

CONCLUSIONS

We presented the use and the validation of a gFET setup design with a coplanar Ag/AgCl gate for monitoring the kinetic adsorption of charged macromolecules. The coplanar gate configuration allowed measuring sequential adsorption processes by washing out and changing the solutions without interrupting the current measurement during the LbL assembly. We employed this procedure to perform a kinetic study of the gFET signal as polyelectrolyte layers were adsorbed and found the same kinetic parameters as those obtained by SPR measurements under the same conditions. The match between the gFET signal and the SPR measurements has been ascribed to the gate geometry and nature, which allows the present device to be capable of performing the very reliable sensing of charged macromolecule adsorption in real time. In addition, comparative monitoring of the adsorption process through the different techniques provided extra information about the gFET sensing system. (i) Charges can be sensed at distances far beyond the solution Debye length through a direct electrostatic mechanism. Thus, polyelectrolyte adsorption could be monitored in real time, in high ionic strength, by simply applying a constant V_{DS} and measuring the output current. (ii) As in many field-effect devices, biasing the gFET through a constant gate potential amplifies the current response, increasing the sensitivity of the device while keeping the kinetic response unaltered. (iii) The changes in I_{DS} caused by the adsorption of each polyelectrolyte layer are lower as the PEM film thickness increases, and this can be interpreted by a simple model based on the Debye–Hückel approximations. The results obtained by combining SPR and EG-gFET measurements quantitatively support a theoretical thermodynamic model previously reported[25] that predicted an increase of 1 order of magnitude in Debye length inside the PEM. Finally, the high reliability of the gFET device for monitoring macromolecule adsorption kinetics demonstrated above, even at ionic strengths near to physiological conditions, together with the low cost of this technology provides a novel insight for the use of gFET devices as miniaturized, fast, precise, and exceptionally available tools for

the study of binding interactions and affinity kinetics that could speed up innovations in the biotechnology field.

■ ASSOCIATED CONTENT

ⓢ Supporting Information

The Supporting Information is available free of charge at https://pubs.acs.org/doi/10.1021/acsaelm.2c00624.

> Full SPR and chronoamperometry experiments of the macromolecule adsorption process, mathematical model of the adsorption kinetic process, detailed information and parameters extracted from that model, mathematical and illustrative description of the potential profile inside the PEM, and a model describing the electrical response as a function of the distance between the multilayer and the graphene surface (PDF)

■ AUTHOR INFORMATION

Corresponding Author

Waldemar A. Marmisollé − *Instituto de Investigaciones Fisicoquímicas Teóricas y Aplicadas (INIFTA, Departamento de Química, Facultad de Ciencias Exactas, Universidad Nacional de La Plata (UNLP), CONICET. 64 and 113, Buenos Aires 1900, Argentina;* orcid.org/0000-0003-0031-5371; Email: wmarmi@inifta.unlp.edu.ar

Authors

Juliana Scotto − *Instituto de Investigaciones Fisicoquímicas Teóricas y Aplicadas (INIFTA, Departamento de Química, Facultad de Ciencias Exactas, Universidad Nacional de La Plata (UNLP), CONICET. 64 and 113, Buenos Aires 1900, Argentina*

Agustín L. Cantillo − *Instituto de Investigaciones Fisicoquímicas Teóricas y Aplicadas (INIFTA, Departamento de Química, Facultad de Ciencias Exactas, Universidad Nacional de La Plata (UNLP), CONICET. 64 and 113, Buenos Aires 1900, Argentina; GISENS BIOTECH, Buenos Aires CP 1195, Argentina*

Esteban Piccinini − *Instituto de Investigaciones Fisicoquímicas Teóricas y Aplicadas (INIFTA, Departamento de Química, Facultad de Ciencias Exactas, Universidad Nacional de La Plata (UNLP), CONICET. 64 and 113, Buenos Aires 1900, Argentina*

Gonzalo E. Fenoy − *Instituto de Investigaciones Fisicoquímicas Teóricas y Aplicadas (INIFTA, Departamento de Química, Facultad de Ciencias Exactas, Universidad Nacional de La Plata (UNLP), CONICET. 64 and 113, Buenos Aires 1900, Argentina;* orcid.org/0000-0003-4336-4843

Juan A. Allegretto − *Instituto de Investigaciones Fisicoquímicas Teóricas y Aplicadas (INIFTA, Departamento de Química, Facultad de Ciencias Exactas, Universidad Nacional de La Plata (UNLP), CONICET. 64 and 113, Buenos Aires 1900, Argentina;* orcid.org/0000-0002-7371-2610

José M. Piccinini − *GISENS BIOTECH, Buenos Aires CP 1195, Argentina*

Omar Azzaroni − *Instituto de Investigaciones Fisicoquímicas Teóricas y Aplicadas (INIFTA, Departamento de Química, Facultad de Ciencias Exactas, Universidad Nacional de La Plata (UNLP), CONICET. 64 and 113, Buenos Aires 1900, Argentina;* orcid.org/0000-0002-5098-0612

Complete contact information is available at:

https://pubs.acs.org/10.1021/acsaelm.2c00624

Author Contributions

§J.S. and A.L.C. are joint first authors.

Author Contributions

The manuscript was written through contributions of all authors. All authors have given approval to the final version of the manuscript.

Notes

The authors declare the following competing financial interest(s): E.P., W.A.M., and O.A. are scientific advisors of GISENS BIOTECH through a contract among UNLP, CONICET, and GISENS BIOTECH. A.L.C. and J.M.P. are recently or presently employed by GISENS BIOTECH. The other authors declare no competing interests.

■ ABBREVIATIONS

gFETs, graphene field-effect transistors; SPR, surface plasmon resonance; BLI, bio layer interferometry; EDL, electrical double layer; PEM, polyelectrolyte multilayer; LbL, layer-by-layer; PDADMAC, poly(diallyldimethylammonium chloride); PSS, poly(styrenesulfonate); rGO, reduced graphene oxide; DMF, dimethylformamide; OC, open circuit; EG, electrolyte gated; CNP, charge neutrality point

■ REFERENCES

(1) Hajian, R.; Balderston, S.; Tran, T.; deBoer, T.; Etienne, J.; Sandhu, M.; Wauford, N. A.; Chung, J. Y.; Nokes, J.; Athaiya, M.; Paredes, J.; Peytavi, R.; Goldsmith, B.; Murthy, N.; Conboy, I. M.; Aran, K. Detection of Unamplified Target Genes via CRISPR–Cas9 Immobilized on a Graphene Field-Effect Transistor. *Nat. Biomed. Eng.* **2019**, *3* (6), 427–437.

(2) Zou, X.; Wu, J.; Gu, J.; Shen, L.; Mao, L. Application of Aptamers in Virus Detection and Antiviral Therapy. *Front. Microbiol.* **2019**, *10*, 1.

(3) Tu, J.; Torrente-Rodríguez, R. M.; Wang, M.; Gao, W. The Era of Digital Health: A Review of Portable and Wearable Affinity Biosensors. *Adv. Funct. Mater.* **2020**, *30* (29), 1906713.

(4) Bhalla, N.; Pan, Y.; Yang, Z.; Payam, A. F. Opportunities and Challenges for Biosensors and Nanoscale Analytical Tools for Pandemics: COVID-19. *ACS Nano* **2020**, *14* (7), 7783–7807.

(5) Renaud, J. P.; Chung, C. W.; Danielson, U. H.; Egner, U.; Hennig, M.; Hubbard, R. E.; Nar, H. Biophysics in Drug Discovery: Impact, Challenges and Opportunities. *Nat. Rev. Drug Discovery* **2016**, *15* (10), 679–698.

(6) Fang, Y. Ligand-Receptor Interaction Platforms and Their Applications for Drug Discovery. *Expert Opin. Drug Discovery* **2012**, *7* (10), 969–988.

(7) Nakatsuka, N.; Yang, K. A.; Abendroth, J. M.; Cheung, K. M.; Xu, X.; Yang, H.; Zhao, C.; Zhu, B.; Rim, Y. S.; Yang, Y.; Weiss, P. S.; Stojanović, M. N.; Andrews, A. M. Aptamer-Field-Effect Transistors Overcome Debye Length Limitations for Small-Molecule Sensing. *Science (80-.)* **2018**, *362* (6412), 319–324.

(8) Saftics, A.; Kurunczi, S.; Peter, B.; Szekacs, I.; Ramsden, J. J.; Horvath, R. Data Evaluation for Surface-Sensitive Label-Free Methods to Obtain Real-Time Kinetic and Structural Information of Thin Films: A Practical Review with Related Software Packages. *Adv. Colloid Interface Sci.* **2021**, *294*, 102431.

(9) Soltermann, F.; Struwe, W. B.; Kukura, P. Label-Free Methods for Optical: In Vitro Characterization of Protein-Protein Interactions. *Phys. Chem. Chem. Phys.* **2021**, *23* (31), 16488–16500.

(10) Dzimianski, J. V.; Lorig-Roach, N.; O'Rourke, S. M.; Alexander, D. L.; Kimmey, J. M.; DuBois, R. M. Rapid and Sensitive Detection of SARS-CoV-2 Antibodies by Biolayer Interferometry. *Sci. Rep.* **2020**, *10* (1), 1–12.

(11) Steinicke, F.; Oltmann-Norden, I.; Wätzig, H. Long Term Kinetic Measurements Revealing Precision and General Performance of Surface Plasmon Resonance Biosensors. *Anal. Biochem.* **2017**, *530*, 94–103.

(12) Tao, Y.; Chen, L.; Pan, M.; Zhu, F.; Zhu, D. Tailored Biosensors for Drug Screening, Efficacy Assessment, and Toxicity Evaluation. *ACS Sensors* **2021**, *6* (9), 3146–3162.

(13) Piccinini, E.; Allegretto, J. A.; Scotto, J.; Cantillo, A. L.; Fenoy, G. E.; Marmisollé, W. A.; Azzaroni, O. Surface Engineering of Graphene through Heterobifunctional Supramolecular-Covalent Scaffolds for Rapid COVID-19 Biomarker Detection. *ACS Appl. Mater. Interfaces* **2021**, *13*, 43696.

(14) Kanai, Y.; Ohmuro-Matsuyama, Y.; Tanioku, M.; Ushiba, S.; Ono, T.; Inoue, K.; Kitaguchi, T.; Kimura, M.; Ueda, H.; Matsumoto, K. Graphene Field Effect Transistor-Based Immunosensor for Ultrasensitive Noncompetitive Detection of Small Antigens. *ACS Sensors* **2020**, *5* (1), 24–28.

(15) Piccinini, E.; Bliem, C.; Reiner-rozman, C.; Battaglini, F.; Azzaroni, O.; Knoll, W. Biosensors and Bioelectronics Enzyme-Polyelectrolyte Multilayer Assemblies on Reduced Graphene Oxide Fi Eld-e Ff Ect Transistors for Biosensing Applications. *Biosens. Bioelectron.* **2016**, *92*, 661–667.

(16) Berninger, T.; Bliem, C.; Piccinini, E.; Azzaroni, O.; Knoll, W. Cascading Reaction of Arginase and Urease on a Graphene-Based FET for Ultrasensitive, Real-Time Detection of Arginine. *Biosens. Bioelectron.* **2018**, *115*, 104–110.

(17) Piccinini, E.; Fenoy, G. E.; Cantillo, A. L.; Allegretto, J. A.; Scotto, J.; Piccinini, J. M.; Marmisollé, W. A.; Azzaroni, O. Biofunctionalization of Graphene-Based FET Sensors through Heterobifunctional Nanoscaffolds: Technology Validation toward Rapid COVID-19 Diagnostics and Monitoring. *Adv. Mater. Interfaces* **2022**, *9* (15), 2102526.

(18) Fenoy, G. E.; Marmisollé, W. A.; Azzaroni, O.; Knoll, W. Acetylcholine Biosensor Based on the Electrochemical Functionalization of Graphene Field-Effect Transistors. *Biosens. Bioelectron.* **2020**, *148*, 111796.

(19) Fenoy, G. E.; Marmisollé, W. A.; Knoll, W.; Azzaroni, O. Highly Sensitive Urine Glucose Detection with Graphene Field-Effect Transistors Functionalized with Electropolymerized Nanofilms. *Sensors & Diagnostics* **2022**, *1* (1), 139–148.

(20) Fu, W.; Jiang, L.; van Geest, E. P.; Lima, L. M. C.; Schneider, G. F. Sensing at the Surface of Graphene Field-Effect Transistors. *Adv. Mater.* **2017**, *29* (6), 1603610.

(21) Hasler, R.; Reiner-Rozman, C.; Fossati, S.; Aspermair, P.; Dostalek, J.; Lee, S.; Ibáñez, M.; Bintinger, J.; Knoll, W. Field-Effect Transistor with a Plasmonic Fiber Optic Gate Electrode as a Multivariable Biosensor Device. *ACS Sensors* **2022**, *7* (2), 504–512.

(22) Xu, S.; Zhan, J.; Man, B.; Jiang, S.; Yue, W.; Gao, S.; Guo, C.; Liu, H.; Li, Z.; Wang, J.; Zhou, Y. Real-Time Reliable Determination of Binding Kinetics of DNA Hybridization Using a Multi-Channel Graphene Biosensor. *Nat. Commun.* **2017**, *8*, 1–10.

(23) Gao, J.; Gao, Y.; Han, Y.; Pang, J.; Wang, C.; Wang, Y.; Liu, H.; Zhang, Y.; Han, L. Ultrasensitive Label-Free MiRNA Sensing Based on a Flexible Graphene Field-Effect Transistor without Functionalization. *ACS Appl. Electron. Mater.* **2020**, *2* (4), 1090–1098.

(24) Gobbi, M.; Galanti, A.; Stoeckel, M. A.; Zyska, B.; Bonacchi, S.; Hecht, S.; Samorì, P. Graphene Transistors for Real-Time Monitoring Molecular Self-Assembly Dynamics. *Nat. Commun.* **2020**, *11* (1), 1–8.

(25) Piccinini, E.; Alberti, S.; Longo, G. S.; Berninger, T.; Breu, J.; Dostalek, J.; Azzaroni, O.; Knoll, W. Pushing the Boundaries of Interfacial Sensitivity in Graphene FET Sensors: Polyelectrolyte Multilayers Strongly Increase the Debye Screening Length. *J. Phys. Chem. C* **2018**, *122* (18), 10181−10188.

(26) Haustein, N.; Gutiérrez-Sanz, Ó.; Tarasov, A. Analytical Model to Describe the Effect of Polyethylene Glycol on Ionic Screening of Analyte Charges in Transistor-Based Immunosensing. *ACS Sensors* **2019**, *4* (4), 874−882.

(27) Gao, N.; Zhou, W.; Jiang, X.; Hong, G.; Fu, T. M.; Lieber, C. M. General Strategy for Biodetection in High Ionic Strength Solutions Using Transistor-Based Nanoelectronic Sensors. *Nano Lett.* **2015**, *15* (3), 2143−2148.

(28) Gao, N.; Gao, T.; Yang, X.; Dai, X.; Zhou, W.; Zhang, A.; Lieber, C. M. Specific Detection of Biomolecules in Physiological Solutions Using Graphene Transistor Biosensors. *Proc. Natl. Acad. Sci. U. S. A.* **2016**, *113* (51), 14633−14638.

(29) Aspermair, P.; Ramach, U.; Reiner-Rozman, C.; Fossati, S.; Lechner, B.; Moya, S. E.; Azzaroni, O.; Dostalek, J.; Szunerits, S.; Knoll, W.; Bintinger, J. Dual Monitoring of Surface Reactions in Real Time by Combined Surface-Plasmon Resonance and Field-Effect Transistor Interrogation. *J. Am. Chem. Soc.* **2020**, *142*, 11709.

(30) Chu, C.-H.; Sarangadharan, I.; Regmi, A.; Chen, Y.-W.; Hsu, C.-P.; Chang, W.-H.; Lee, G.-Y.; Chyi, J.-I.; Chen, C.-C.; Shiesh, S.-C.; Lee, G.-B.; Wang, Y.-L. Beyond the Debye Length in High Ionic Strength Solution: Direct Protein Detection with Field-Effect Transistors (FETs) in Human Serum. *Sci. Rep.* **2017**, *7* (1), 1−15.

(31) Cicoira, F.; Sessolo, M.; Yaghmazadeh, O.; Defranco, J. A.; Yang, S. Y.; Malliaras, G. C. Influence of Device Geometry on Sensor Characteristics of Planar Organic Electrochemical Transistors. *Adv. Mater.* **2010**, *22* (9), 1012−1016.

(32) Chen, T. Y.; Loan, P. T. K.; Hsu, C. L.; Lee, Y. H.; Tse-Wei Wang, J.; Wei, K. H.; Lin, C. Te; Li, L. J. Label-Free Detection of DNA Hybridization Using Transistors Based on CVD Grown Graphene. *Biosens. Bioelectron.* **2013**, *41* (1), 103−109.

(33) Bliem, C.; Piccinini, E.; Knoll, W.; Azzaroni, O. *Enzyme Multilayers on Graphene-Based FETs for Biosensing Applications*, 1st ed.; Elsevier: 2018; Vol. *609*. DOI: 10.1016/bs.mie.2018.06.001.

(34) Piccinini, J. M.; Azzaroni, O.; Piccinini, E.; Marmisolle, W. A.; Allegretto, J. A.; Scotto, J.; Cantillo, A. L.; Fenoy, G. E. WO 2021240440A1, 2021.

(35) Guzmán, E.; Ritacco, H.; Ortega, F.; Rubio, R. G. Evidence of the Influence of Adsorption Kinetics on the Internal Reorganization of Polyelectrolyte Multilayers. *Colloids Surfaces A Physicochem. Eng. Asp.* **2011**, *384* (1−3), 274−281.

(36) Guzmán, E.; Ritacco, H.; Ortega, F.; Svitova, T.; Radke, C. J.; Rubio, R. G. Adsorption Kinetics and Mechanical Properties of Ultrathin Polyelectrolyte Multilayers: Liquid-Supported versus Solid-Supported Films. *J. Phys. Chem. B* **2009**, *113* (20), 7128−7137.

(37) Maza, E.; Tuninetti, J. S.; Politakos, N.; Knoll, W.; Moya, S.; Azzaroni, O. PH-Responsive Ion Transport in Polyelectrolyte Multilayers of Poly(Diallyldimethylammonium Chloride) (PDAD-MAC) and Poly(4-Styrenesulfonic Acid-Co-Maleic Acid) (PSS-MA) Bearing Strong- and Weak Anionic Groups. *Phys. Chem. Chem. Phys.* **2015**, *17* (44), 29935−29948.

(38) Picart, C.; Mutterer, J.; Richert, L.; Luo, Y.; Prestwich, G. D.; Schaaf, P.; Voegel, J. C.; Lavalle, P. Molecular Basis for the Explanation of the Exponential Growth of Polyelectrolyte Multilayers. *Proc. Natl. Acad. Sci. U. S. A.* **2002**, *99* (20), 12531−12535.

(39) Wang, Y. Y.; Burke, P. J. Polyelectrolyte Multilayer Electrostatic Gating of Graphene Field-Effect Transistors. *Nano Res.* **2014**, *7* (11), 1650−1658.

(40) Kovacevic, D.; Van der Burgh, S.; De Keizer, A.; Cohen Stuart, M. A. Kinetics of Formation and Dissolution of Weak Polyelectrolyte Multilayers: Role of Salt and Free Polyions. *Langmuir* **2002**, *18* (14), 5607−5612.

(41) Liang, Y.; Gao, F.; Wang, L.; Lin, S. In-Situ Monitoring of Polyelectrolytes Adsorption Kinetics by Electrochemical Impedance Spectroscopy: Application in Fabricating Nanofiltration Membranes via Layer-by-Layer Deposition. *J. Membr. Sci.* **2021**, *619*, 118747.

(42) Sill, A.; Nestler, P.; Weltmeyer, A.; Paßvogel, M.; Neuber, S.; Helm, C. A. Polyelectrolyte Multilayer Films from Mixtures of Polyanions: Different Compositions in Films and Deposition Solutions. *Macromolecules* **2020**, *53* (16), 7107−7118.

(43) Fares, H. M.; Schlenoff, J. B. Diffusion of Sites versus Polymers in Polyelectrolyte Complexes and Multilayers. *J. Am. Chem. Soc.* **2017**, *139* (41), 14656−14667.

(44) Salehi, A.; Desai, P. S.; Li, J.; Steele, C. A.; Larson, R. G. Relationship between Polyelectrolyte Bulk Complexation and Kinetics of Their Layer-by-Layer Assembly. *Macromolecules* **2015**, *48* (2), 400−409.

(45) Kesler, V.; Murmann, B.; Soh, H. T. Going beyond the Debye Length: Overcoming Charge Screening Limitations in Next-Generation Bioelectronic Sensors. *ACS Nano* **2020**, *14* (12), 16194−16201.

(46) Ohno, Y.; Maehashi, K.; Matsumoto, K. Label-Free Biosensors Based on Aptamer-Modified Graphene Field-Effect. *J. Am. Chem. Soc.* **2010**, *132*, 18012−18013.

(47) Wang, X.; Zhu, Y.; Olsen, T. R.; Sun, N.; Zhang, W.; Pei, R.; Lin, Q. A Graphene Aptasensor for Biomarker Detection in Human Serum. *Electrochim. Acta* **2018**, *290*, 356−363.

(48) Filipiak, M. S.; Rother, M.; Andoy, N. M.; Knudsen, A. C.; Grimm, S.; Bachran, C.; Swee, L. K.; Zaumseil, J.; Tarasov, A. Highly Sensitive, Selective and Label-Free Protein Detection in Physiological Solutions Using Carbon Nanotube Transistors with Nanobody Receptors. *Sensors Actuators, B Chem.* **2018**, *255*, 1507−1516.

(49) Hideshima, S.; Sato, R.; Inoue, S.; Kuroiwa, S.; Osaka, T. Detection of Tumor Marker in Blood Serum Using Antibody-Modified Field Effect Transistor with Optimized BSA Blocking. *Sensors Actuators, B Chem.* **2012**, *161* (1), 146−150.